The critical exponent of binary liquid mixtures by Rayleigh and Brillouin scattering measurements: the hexane-methanol system

The critical exponent of binary liquid mixtures by Rayleigh and Brillouin scattering measurements: The hexane–methanol system

S Kawase†, K Maruyama‡, S Tamaki§ and H Okazaki§

† College of Biomedical Technology, Niigata University, Asahimachi-dori, Niigata 951, Japan
‡ Department of Chemistry, Faculty of Science, Niigata University, Igarashi, Niigata 950-21, Japan
§ Department of Physics, Faculty of Science, Niigata University, Igarashi, Niigata 950-21, Japan

Abstract. The Rayleigh and Brillouin scattering has been investigated for the hexane–methanol system at several compositions near their consolute temperatures from one phase to two phases, and some thermodynamical properties such as a ratio of specific heats C_p/C_v, a concentration-concentration fluctuation $S_{cc}(0)$, and the correlation length ξ have been derived. The total scattering intensity and therefore $S_{cc}(0)$ diverge at the spinodal temperature for all samples. However, the critical index depends on the composition. This phenomenon has been analysed in terms of a modified Flory approximation, in which we have assumed that a repulsive term of the interaction varies with temperature. The consolute and spinodal temperatures were estimated. The Brillouin shift and corresponding sound velocity have no anomaly near these consolute temperatures.

1. Introduction

In previous papers [1, 2], we have found that the Rayleigh and Brillouin scattering intensities of the binary fluid system could be described in terms of Bhatia–Thornton [3] type fluctuations in the long-wavelength limit, by performing experiments of Rayleigh–Brillouin scattering for hexane–methanol (C_6H_{14}–CH_3OH) and cyclohexane–methanol (C_6H_{12}–CH_3OH) solutions, both of which have miscibility gaps in their T–c phase diagrams. The light scattering from a monatomic liquid is fully explained the hydrodynamic form of the Van Hove space–time correlation function, $S(\omega, q)$. Moreover, the total integrated intensity, $\mathcal{I}_R + 2\mathcal{I}_B$, of the Rayleigh peak and the Brillouin doublet is proportional to the structure factor, $S(q)$, and is written as [4–6]

$$\mathcal{I}_R + 2\mathcal{I}_B = C\alpha^2 S(q) \tag{1}$$

where C is given by the experimental situation, q is the momentum transfer of incident light and α is the polarizability of the molecule forming its liquid. The extension of equation (1) to a binary fluid is straightforward and has been shown in previous papers [1, 2].

Experimental study on the critical exponents for the gas–liquid transition has been reported by several workers [7–18] and some of these have already been cited in a text book [19] and monographs [9, 20–22]. For liquid–liquid transitions such as that from one phase to two other phases, however, the experimental results of Rayleigh–Brillouin scattering reported to date are rare [23]. Recently Bot and Wegdam [24], however, investigated the

Rayleigh–Brillouin scattering from gas mixtures using Faber–Ziman partial structure factors. In addition to this, our previous experiments have shown that the major contribution of the Rayleigh–Brillouin scattering is due to the concentration–concentration fluctuation in the long-wavelength limit and all data for such liquids including those with a miscibility gap are interpreted in terms of a modified Flory approximation [25]. These situations prompted us to perform experiments on the behaviour of Rayleigh–Brillouin scattering near the critical temperature T_c of transition from one phase to two other phases.

In a previous paper [26] we carried out Rayleigh–Brillouin measurements for cyclohexane–methanol mixtures. The spinodal temperatures, where the concentration fluctuation $S_{cc}(0)$ diverges, could be estimated from the total scattering intensity. Furthermore, other data such as specific-heat ratio and sound velocity were derived from Brillouin doublet spectra. However since the intensity of the Brillouin doublet is very weak in this system, it was difficult to obtain precise data near the critical temperature.

In this work, we selected hexane–methanol mixtures as samples because they show a sufficiently large Brillouin doublet. Therefore we could analyse both the Rayleigh line and the Brillouin doublet with high accuracy even near the transition temperature. We report detailed results of the Rayleigh–Brillouin scattering for C_6H_{12}–CH_3OH mixtures and the critical behaviour of some thermodynamic quantities, such as the concentration–concentration fluctuation $S_{cc}(0)$, the specific-heat ratio C_p/C_v, the adiabatic compressibility χ_s and the correlation length ξ.

2. Experimental details

A detailed description of the apparatus for Rayleigh–Brillouin spectroscopy was presented in previous papers [1, 2]. The brief description of the instrument is as follows. The light source is a 500 mW argon-ion laser ($\lambda = 514.5$ nm). The incident-light power was adjusted by ND filters and was monitored with a photodiode cell. A sample was set in a water-flow cryostat and the temperature was controlled with deviation less than 0.02 °C over the range of 40–75 °C. The light scattered at right angles is analysed by a monochromator with a resolution of 0.28 nm and a Fabry–Pérot interferometer, and detected by a photomultiplier. The overall instrumental half width is about 0.015 cm^{-1}.

The samples used in the present experiment were commercially available reagents, with 99.9 mol.% purity, and their mixtures, and were made dust free by using a membrane filter (Advantec, Dismic) with a pore size of 0.2 μm. The test of a solution being dust free was done by comparing the observed Rayleigh spectrum with the cited one of a dust-free sample. The mixed sample set in a measurement cell was heated up to a temperature higher than the one-phase-to-two-phases transition temperature by 20 °C, then was shaken to make it a uniform fluid. After that the measurements were performed decreasing the temperature step by step.

3. Results

Figure 1 shows a phase diagram of the C_6H_{14}–CH_3OH system. The open circles are the consolute points. As seen in this figure, this system has a critical point at 34.58 °C at the equimolar composition. Therefore we have performed measurements of the equimolar mixture first.

Figure 2 shows Rayleigh–Brillouin scattering spectra observed at several temperatures, where the intensity was normalized by incident-light intensity. The intensities of the
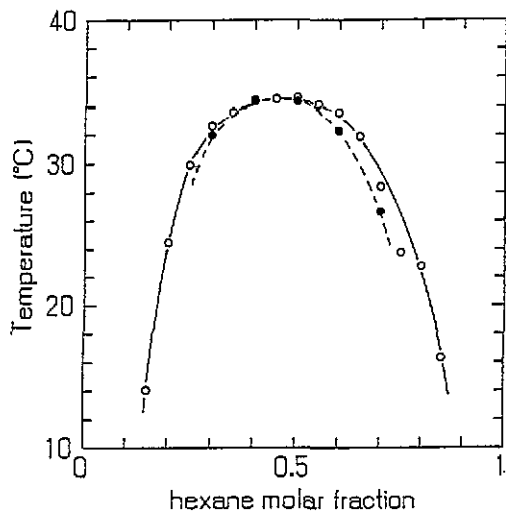
Figure 1. A phase diagram of the C_6H_{14}–CH_3OH system [2]. The open circles denote the consolute points and the closed circles the estimated spinodal temperatures. The solid and broken lines are guides for the eyes.
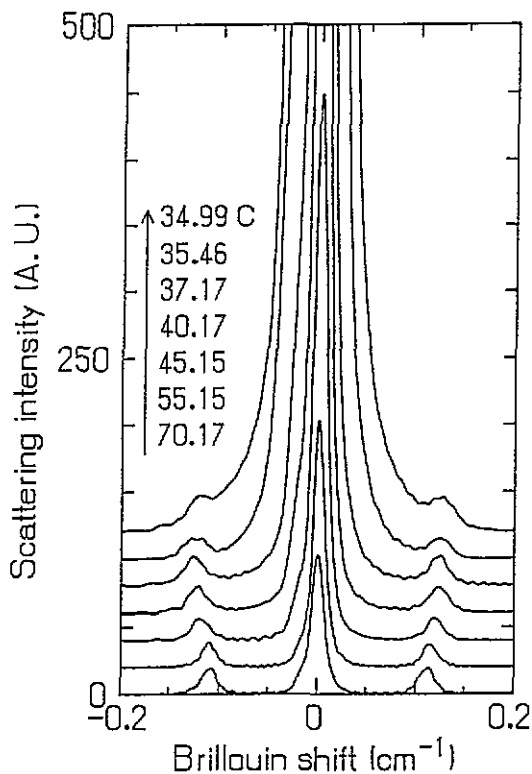

Figure 2. Observed Rayleigh and Brillouin spectra for a C_6H_{14}–CH_3OH equicomponent mixture at several temperatures.

Brillouin doublet are so large as to be analysed with a high accuracy even near the critical temperature. The intensity of the Rayleigh line rapidly increases when temperature decreases and it seems to diverge near the critical temperature. On the other hand, the intensity of the Brillouin doublet seems to be hardly changed, and the Brillouin shift becomes slightly larger.

Figure 3 shows a log–log plot of the total scattering intensity, which is calculated from the area under the spectrum, $\mathcal{I}$ ($= \mathcal{I}_R + 2\mathcal{I}_B$), as a function of $T - T_c$. The intensity seems
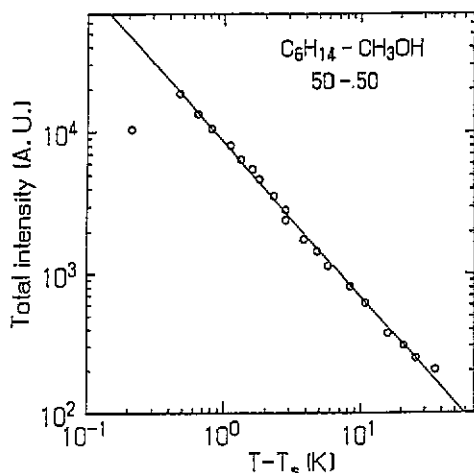
Figure 3. A log–log plot of the total scattering intensity against $T - T_c$. The solid line represents the power law $\mathcal{I} \sim (T - T_c)^{-1.09}$.
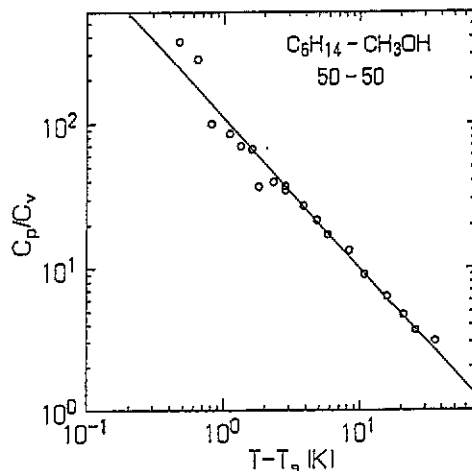
Figure 4. The specific-heat ratio C_p/C_v derived from the Landau–Placzek ratio $\mathcal{I}_R/2\mathcal{I}_B$ as a function of $T - T_c$. The solid line represents the power law $\mathcal{I}_R/2\mathcal{I}_B \sim (T - T_c)^{-1.04}$.

to obey a power law $\mathcal{I} \sim (T - T_c)^{-\gamma}$ except near the critical region, where the scattering intensity seems to be dimmed by multiple scattering. By a least-squares fitting, the critical exponent γ was obtained to be 1.09 ± 0.03. The error of the index was estimated from the change of fitting quality with varying index.

The ratio of the intensity of the Rayleigh line $\mathcal{I}_R$ to that of the Brillouin doublet $2\mathcal{I}_B$ is called the Landau–Placzek ratio and is related to the specific-heat ratio by $C_p/C_v - 1$. The intensity of the Brillouin doublet is separated from that of the Rayleigh line by using least-squares fitting. Figure 4 shows the obtained C_p/C_v as a function of $T - T_c$, and indicates that C_p/C_v also obeys a power law with a critical exponent of about 1.04 ± 0.03.

Figure 5 shows a Brillouin shift as a function of $T - T_c$. The Brillouin shift slightly increases with decreasing temperature. However, no anomaly can be observed even near the critical temperature. The sound velocity in the liquid is related to the Brillouin shift $\Delta\omega$ by

$$\Delta\omega/\omega = (2nv_s/c)\sin(\theta/2) \qquad (\theta = 90°) \qquad (2)$$

where n is the refractive index and ω is the frequency of the incident light. The values of n used were taken from [27] and are listed in table 1. In figure 5 the corresponding sound velocity is indicated on the right-hand side.

For the non-equicomponent mixtures the consolute temperature T_c is expected to be different from the spinodal temperature T_s, where the concentration–concentration fluctuation $S_{cc}(0)$ $(= Nk_BT(\partial^2 G/\partial c^2)^{-1})$ diverges. Therefore it is interesting to study the difference of behaviour of the thermodynamic quantities from the equicomponent mixture.

Hence we have also performed scattering measurements for non-equimolar mixtures (C_6H_{14} molar fraction $c = 0.3, 0.4, 0.6, 0.7$). The total scattering intensity becomes larger at lower temperature and shows the largest value near the consolute transition temperature. However the total intensity does not obey a power law of $T - T_c$, and the temperature of divergence seems to be lower than T_c. Figure 6 shows a log–log plot of the total intensity as a function of $T - T_s$ for several compositions, where T_s was decided so that the experimental
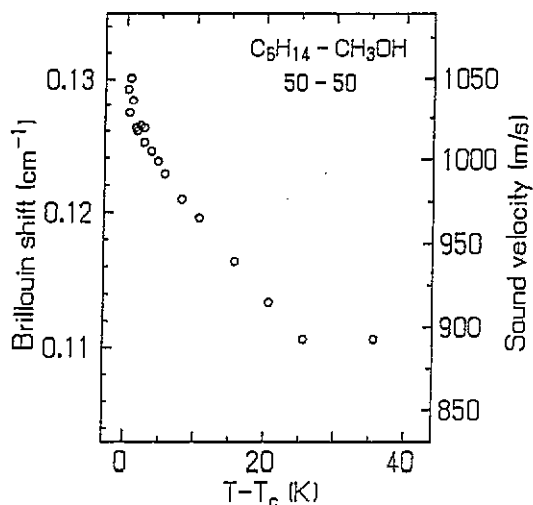
Figure 5. The observed Brillouin shift as a function of $T - T_c$. The corresponding sound velocity is indicated on the right-hand side.

Table 1. The transition temperature from one phase to two phases T_c, the estimated spinodal temperature T_s, the power index of total light scattering intensity γ, that of specific-heat ratio δ, and refractive index n. The errors in temperatures are estimated to be about 0.05 °C and those in indices γ and δ are about 0.03.

Hexane molar fraction	T_c (°C)	T_s (°C)	γ	δ	n
0.3	32.62	31.98	0.69	0.68	1.361
0.4	34.34	34.43	0.95	0.92	1.357
0.5	34.58	34.34	1.09	1.04	1.352
0.6	33.60	32.29	0.60	0.68	1.347
0.7	28.44	26.67	0.22	0.28	1.343

data fitted the power law best. As seen in this figure, the experimental data obey the power law well. Since $S_{cc}(0)$, to which the total intensity is proportional, diverges at the spinodal temperature, the obtained T_s is expected to be equal to the spinodal temperature. The consolute transition temperature T_c, the estimated spinodal temperature T_s and the power index γ are listed in table 1. T_s values are also shown in figure 1 by the closed circles. Figure 7 plots the obtained power index as a function of C_6H_{14} molar fraction. The power index is about unity for the mixture with a hexane molar fraction of 40% and those for other samples are less than unity.

Figure 8 shows the temperature dependence of the specific-heat ratio for non-equimolar-composition samples as a function of $T - T_s$. This also obeys the power law and the power index has the same composition dependence as that of the total scattering intensity. The power index is also listed in table 1.

Figure 9 shows the Brillouin shift as a function of $T - T_c$. The Brillouin shift slightly increases with decreasing temperature. However, no anomaly can be observed near the critical temperature as for the equicomponent mixture. The corresponding sound velocity is shown on the right-hand axis, though the values include a small error from the change of refractive index of the mixture.

4. Discussion

4.1. Total scattering intensity

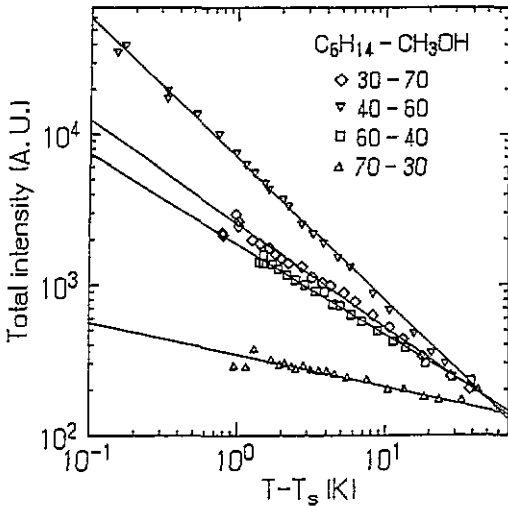The total scattering intensity of binary liquid mixtures can be derived from the modified

Figure 6. A log–log plot of the total scattering intensity against $T - T_s$ for several non-equimolar samples. The lines represent the power law obtained by least-squares fitting.
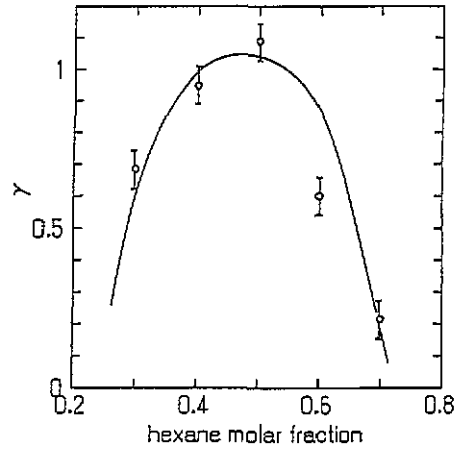

Figure 7. The critical exponent of C_6H_{14}–CH_3OH mixtures of several compositions as a function of the C_6H_{14} molar fraction. The curve is a guide for the eyes.
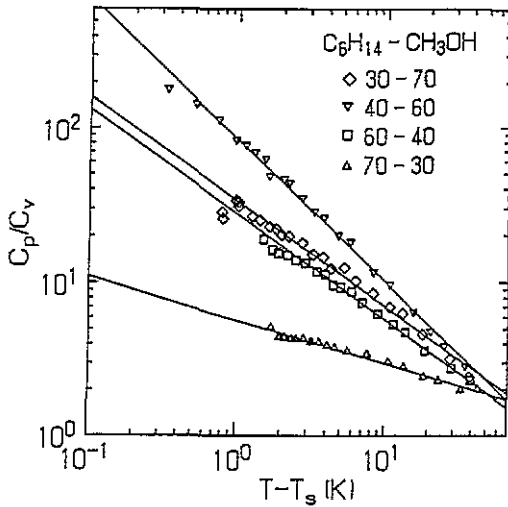

Figure 8. The specific-heat ratio C_p/C_v for several compositions derived from the Landau–Placzek ratio $\mathcal{I}_R/2\mathcal{I}_B$ as a function of $T - T_s$.

conformal solution (MCS) theory by using Bhatia–Thornton structure factors. Here is a brief description of the derivation; a more detailed explanation is to be found elsewhere [25].

The concentration–concentration fluctuation in the long-wavelength limit, $S_{cc}(0, c, T)$, defined by Bhatia and Thornton (BT) is equal to [3]

$$S_{cc}(0, c, T) = Nk_B T \bigg/ \left(\frac{\partial^2 G}{\partial c^2} \right)_{N,p,T}$$

$$= c(1 - c)[1 + c(1 - c)\partial^2 + c(1 - c)g''(c)w/k_B T]^{-1} \qquad (3)$$

where

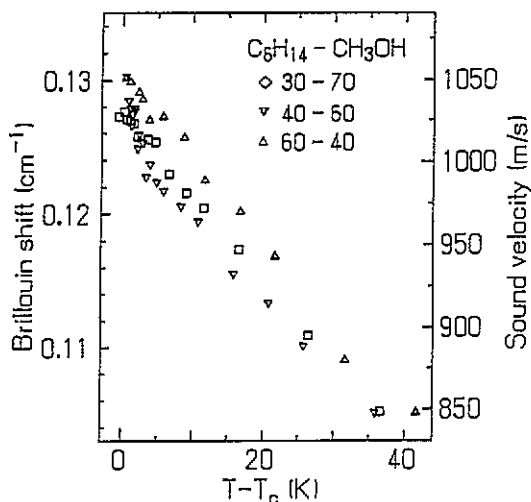$$\delta = (1/V)(\partial V/\partial c)_{N,p,T} \qquad (4)$$

Figure 9. The observed Brillouin shift as a function of $T - T_c$. The corresponding sound velocity is indicated on the right-hand side.

and $g''(c)w$ is the interaction parameter of the Flory model and is assumed to be a function of the concentration.

According to Komarov and Fisher [5], the total scattering intensity $\mathcal{I}$ from a fluid, per unit incident intensity, per unit solid angle, is given by equation (1).

For binary mixtures, the factor $\alpha^2 S(0)$ in equation (1) is expressed as follows by the isothermal compressibility χ_T and the concentration–concentration fluctuation $S_{cc}(0)$ [28]

$$\mathcal{I} = K \langle\!\langle \alpha \rangle\!\rangle^2 [(Nk_B T/V_M)\chi_T + S_{cc}(0, c, T)(\delta - (\alpha_A - \alpha_B)/\langle\!\langle \alpha \rangle\!\rangle)^2] \tag{5}$$

where α_i is the polarizability of component i and $\langle\!\langle \alpha \rangle\!\rangle$ means $c_1\alpha_1 + c_2\alpha_2$. From equations (3) and (5), the total scattering intensity of a binary mixture is given as

$$\mathcal{I} = K \langle\!\langle \alpha \rangle\!\rangle^2 \{(Nk_B T/V_M)\chi_T + [c(1 - c)(\delta - (\alpha_A - \alpha_B)/\langle\!\langle \alpha \rangle\!\rangle)^2]$$
$$\times [1 + c(1 - c)\delta^2 + c(1 - c)g''(c)w/k_B T]^{-1}\}. \tag{6}$$

At the spinodal temperature T_s, since $(\partial^2 G/\partial c^2) = 0$, $S_{cc}(0)$ should diverge to infinity, hence the denominator of the second term of equation (6) is equal to zero. By substituting $1 + c(1 - c)\delta^2 + c(1 - c)g''(c)w/k_B T_s = 0$ into equation (6), we obtain

$$\mathcal{I} = K \langle\!\langle \alpha \rangle\!\rangle^2 [(Nk_B T/V_M)\chi_T + c(1 - c)(\delta - (\alpha_A - \alpha_B)/\langle\!\langle \alpha \rangle\!\rangle)^2/(1 + c(1 - c)\delta^2)(1 - T_s/T)]. \tag{7}$$

The second term of equation (7) diverges as $(T - T_s)^{-1}$ near the critical point; in other words, under the Flory approximation the total light-scattering intensity has a critical exponent $\gamma = 1$ if the value of the first term is negligibly small. The obtained critical exponent for an equimolar mixture (~ 1.09) agrees well with this result.

On the other hand, there is a discrepancy between the results from equation (7) and the experimental results for non-molar mixtures, which are nearly the same as those for the C_6H_{12}–CH_3OH system. To explain this phenomenon the interaction parameter in equation (3), $g(c)w$, must depend on temperature as

$$1 - W/k_B T = (1 - T_s/T)^\gamma \tag{8}$$

where $W = -c(1 - c)g''(c)w/(1 + c(1 - c)\delta^2)$, which represents the temperature dependence of $g''(c)w$. From equation (8) W is obtained to be $k_B T_s$ at the spinodal temperature, and at
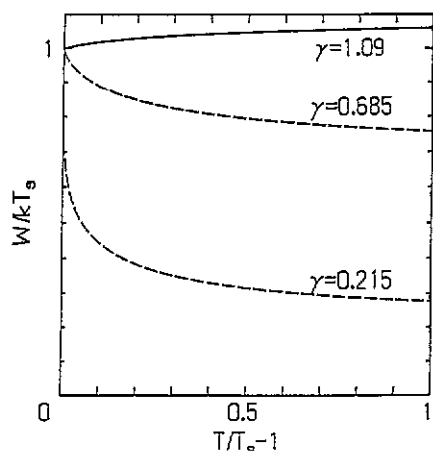
Figure 10. The temperature dependence of W for an equicomponent sample (solid line), and C_6H_{14} 30 and 70 mol% samples (broken lines).
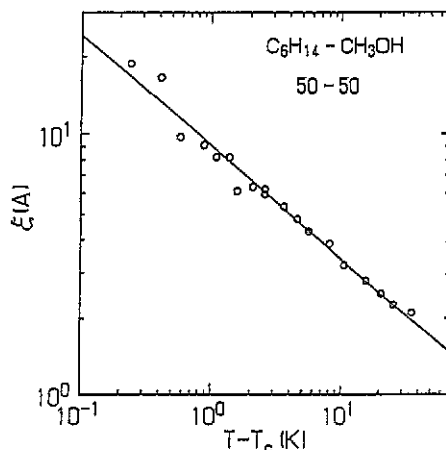
Figure 11. A log–log plot of the correlation length against $T - T_c$ for an equimolar sample. The line represents the power law obtained by least-squares fitting.

higher temperatures ($T \gg T_s, T_c$), W approaches $\gamma k_B T_s$. Figure 10 shows the temperature dependence of W for various samples. This result suggests that a C_6H_{14}–CH_3OH mixture of non-equimolar concentration has a large mixing tendency at higher temperatures compared with that near the critical temperature.

Equation (8) also indicates that for $\gamma < 1$, W has an infinite derivative at the temperature $T = T_s$, which may correspond to the observed phenomenon that non-equimolar samples become cloudy very suddenly at the critical temperature in comparison with the equimolar sample, of which W is nearly independent of temperature. The cause of the temperature dependence of the interaction parameter and the non-unity value of γ is not clear at the present stage of investigation. One possible explanation of this phenomenon is as follows. The orientational configuration between component molecules is very changeable for non-equimolar mixtures because the molecules of the minor component are surrounded by more opponent molecules than in the equimolar mixture. This difference may cause the change of interaction between the components with temperature variation.

4.2. Specific-heat ratio and sound velocity

The value of C_p/C_v at $T - T_s = 50\,°C$ is about 2.0, which is a reasonable value for usual liquids. As seen in figure 4, the specific-heat ratio C_p/C_v diverges at the critical temperature as $(T - T_c)^{-1.04}$ for the equicomponent sample. This result is nearly the same as that for the C_6H_{12}–CH_3OH system and also matches the prediction by the three-dimensional Ising model. Another sample with 40% C_6H_{14} molar fraction also has nearly the same power index (0.95).

On the other hand, C_p/C_v ratios for other samples show slower divergence than that of these two samples does.

The sound velocity in liquid v_s is given as

$$v_s^2 = C_p/\rho C_v \chi_T \tag{9}$$

where ρ is the density and χ_T is the isothermal compressibility. Since χ_T has the same critical index as C_p, v_s has a behaviour near the critical point of $v_s \sim (T/T_c - 1)^{+\alpha/2}$.

From the three-dimensional Ising model, which could be applicable to the present system, $\alpha/2$ is very small (~ 0.05), therefore the experimental result that there is no anomaly near the critical temperature in the sound velocity is inconsistent with the critical theory of gas–liquid transitions. Nearly the same results were obtained by ultrasonic studies for the 3-methylpentane–nitroethane system [29, 30].

4.3. Correlation length

Cannel and Benedek [15] derived the correlation length ξ of Xe near its critical point from the light-scattering data by using the Ornstein–Zernike model. So we also tried to estimate the correlation length of C_6H_{14}–CH_3OH mixtures. The values of C_p/C_v and the correlation length ξ have a relation

$$C_p/C_v = [C_p(q, \omega)/C_v(q, \omega)](1 + q^2\xi^2)v_{00}^2/v_0^2 \tag{10}$$

where $C_p(q, \omega)$ and $C_v(q, \omega)$ are specific heats corresponding to finite q and ξ, C_p and C_v are the quantities with $q = 0$, $\omega = 0$, v_0 is the sound velocity at frequency ω, v_{00} is the true zero-frequency sound velocity ($= (\rho\chi_s)^{-1/2}$). The static C_p/C_v has a relation to the isothermal compressibility χ_T of $C_p = C_v\chi_T/\chi_s$, and χ_T has the relation $\chi_T/\chi_1 = \xi^2/R^2$ where $\chi_1 = 1/nk_BT$ is the isothermal compressibility of an ideal gas of number density n and R is the direct correlation range closely related to the average interatomic distance. In this study the value of 4.9 Å is used for R, which is the atomic distance estimated from the number density. Finally we find

$$\xi^2/R^2 = [C_p(q, \omega)/C_v(q, \omega)][(1 + q^2\xi^2)/\rho v_0^2]nk_BT. \tag{11}$$

By resolving this equation using experimental data for C_p/C_v and v_0, we can obtain the correlation length ξ.

Figure 11 shows the obtained correlation length as a function of $T - T_c$ for the equicomponent mixture. ξ is a few ångströms at a temperature 30 °C higher than T_c and increases to about 20 Å at $T - T_c = 0.2$ °C. These values agree very well with the results for the gas–liquid transition of Xe. From the obtained ξ and momentum transfer q, the maximum value of $q\xi$ is about $5 \times 10^{-2} \ll 1$. This result justifies the hydrodynamic treatment of Brillouin scattering in subsections 4.1 and 4.2. The critical index of ξ obtained by a least-squares fit is 0.43, which is slightly smaller than that of the three-dimensional Ising model (0.63).

5. Summary

Measurements of Rayleigh and Brillouin scattering of C_6H_{14}–CH_3OH solutions have been performed near their one-phase-to-two-phases transition temperature. For a sample of critical composition, the total light-scattering intensity diverges at the critical temperature with a critical exponent of 1.09 ± 0.03. This value is nearly the same as that expected from the Flory approximation. On the other hand, for samples of other compositions the critical exponent is smaller than unity. To explain this phenomenon the Flory approximation was modified so that the repulsive term in the interaction has a temperature dependence. This modification shows that the repulsive term becomes smaller at higher temperatures for non-equimolar-composition samples.

The spinodal temperature, where $\partial^2 G/\partial c^2 = 0$, is estimated from the total scattering intensity. The Brillouin shift and corresponding sound velocity have no anomaly near the transition temperature. Near the transition temperature the Brillouin doublet cannot be observed clearly because of a very strong Rayleigh peak in the present stage of investigation.

Acknowledgments

References

[1] Kawase S, Maruyama K and Okazaki H 1994 *J. Phys.: Condens. Matter* 6 4287
[2] Kawase S, Maruyama K, Tamaki S and Okazaki H 1994 *Phys. Chem. Liq.* 27 49
[3] Bhatia A B and Thornton D E 1970 *Phys. Rev.* B 2 3004
[4] Van Hove L 1954 *Phys. Rev.* 95 249
[5] Komarov L I and Fisher I Z 1963 *Sov. Phys.–JETP* 16 1358
[6] Bhatia A B and Tong E 1968 *Phys. Rev.* 173 231
[7] Gammon R W, Swinney H L and Cummins H Z 1967 *Phys. Rev. Lett.* 19 1467
[8] Ford N C Jr, Langley K H and Puglielli V G 1968 *Phys. Rev. Lett.* 21 9
[9] Mountain R D 1969 *J. Res. NBS* A 73 593
[10] Eden D, Garland C W and Thoen J 1972 *Phys. Rev. Lett.* 28 726
[11] Baharudin B Y, Jackson D A and Schoen P E 1973 *Phys. Lett.* 46A 39
[12] Eden D and Swinney H L 1974 *Opt. Commun.* 10 191
[13] Aref'ev I M and Fabelinskii I L 1973 *Opt. Commun.* 9 69
[14] Aref'ev I M 1974 *Opt. Commun.* 10 277
[15] Cannel D S and Benedek G B 1970 *Phys. Rev. Lett.* 25 1157
[16] Garland C W, Eden D and Mistura L 1970 *Phys. Rev. Lett.* 25 1161
[17] Cummins H Z and Swinney H L 1970 *Phys. Rev. Lett.* 25 1165
[18] Henry D L, Swinney H L and Cummins H Z 1970 *Phys. Rev. Lett.* 25 1170
[19] Stanley H E 1971 *Introduction to Phase Transitions and Critical Phenomena* (London: Oxford University Press) ch 14
[20] Fisher M E 1964 *J. Math. Phys.* 5 66
[21] Kadanoff L P, Götze W, Hamblen D, Hecht R, Lewis E A S, Palciauskas V V, Payl M, Swift J, Aspnes D and Kane J 1967 *Rev. Mod. Phys.* 39 397
[22] Tisza L 1961 *Ann. Phys., NY* 13 1
[23] Polensky N and Chen S H 1968 *Phys. Rev. Lett.* 20 909
[24] Bot A and Wegdam G H 1991 *J. Phys. Chem.* 95 4679
[25] Flory P J 1942 *J. Chem. Phys.* 10 51
[26] Kawase S, Maruyama K, Tamaki S and Okazaki H in preparation
[27] Miller T M 1988 *Handbook of Chemistry and Physics* 6th edn, ed R C West (Boca Raton, FL: Chemical Rubber Company) p E68
[28] Cusack N E 1987 *The Physics of Structurally Disordered Matter* (Bristol: Hilger) ch 3
[29] Garland C W and Sanchez G 1983 *J. Chem. Phys.* 79 3090
[30] Sanchez G and Garland C W 1983 *J. Chem. Phys.* 79 3100